DESIGN OF A PLANAR META-SURFACE BASED ON DIPOLES AND WIRES FOR ANTENNA APPLICATIONS

E. Saenz[1], R. Gonzalo[1], I. Ederra[1], and P. de Maagt[2]

[1]*Electrical and Electronic Engineering Department, Public University of Navarra, Campus Arrosadia E-31006 Pamplona-Navarra, (Spain), Email: elena.saenz@unavarra.es, ramon@unavara.es, inigo.ederra@unavarra.es*
[2]*Electromagnetics & Space Environments Division, ESTEC, PO Box 299, 2200 AG, Noordwijk, (The Netherlands), Email: Peter.de.Maagt@esa.int*

ABSTRACT

In this paper, the design of a planar meta-surface based on dipoles and wires is presented. The unit cell is formed by three independent layers, which contain two parallel dipoles and one wire. The behaviour of these elements have been analysed separately as an independent unit cell, i.e., the one dipole unit cell, the two dipoles unit cell and the two dipoles and wire unit cell, by means of the transmission response and the dispersion diagrams. For a normal incident plane wave with the E field parallel to the wires and the H field axial to the dipoles, the electric and magnetic responses are excited producing a pass band behaviour which exhibit negative refractive index. This cell has been used to create meta-surfaces for antenna applications. Two configurations have been analysed; the first one is a superstrate of a dipole antenna with the pass band tuned to the resonant frequency of the dipole. It has been observed that the power goes through the meta-surface and is radiated mainly in boresight direction, which increases the directivity up to 8 dBi and the aperture efficiency of the whole configuration. In the second case, a substrate with the stop band tuned to the pass band of the superstrate and the resonant frequency of the dipole has been added. A directivity higher than 9 dBi with a back radiation of -20 dBi have been obtained.

Key words: Metamaterial; Meta-surface; Enhanced directivity.

1. INTRODUCTION

Since Veselago suggested the possibility of Left Handed materials (LHM) [1], many implementations of them have been carried out demonstrating the existence these negative index materials (NIM). The first demonstration was done by the UCSD group in 2000 [2] and after that, most of them have been based on the topology proposed by Pendry [3]. By combining properly Split Ring Resonators (SRRs), or negative permeability elements ($\mu < 0$) and continuous wires, or negative permittivity elements ($\varepsilon < 0$), both magnitudes will be simultaneously negative achieving the effective negative refractive index.

In order to excite correctly the unit cell, a plane wave with the E field parallel to the wires and H field axial to the SRR is required, which means a propagation vector parallel to the SRR plane. This fixed polarization makes it very difficult to measure the transmission and reflection coefficients, which are essential to characterize the structure.

Due to these practical problems, alternative configurations based on short wire pairs have been designed by different authors [4]-[5]. These new planar structures are easier to fabricate and characterize by measuring the transmission and reflection coefficients. The main idea is to replace the conventional SRR by two parallel wires that produce the same effect, an inductance L and capacitance C with a resonant frequency $\omega = 1/\sqrt{LC}$. Working around the resonant frequency, the magnetic and electric resonance will be excited obtaining a negative refractive index. Although theoretically only the wire pairs are enough to obtain the negative refraction index, in practice [5] it is required to provide extra negative permittivity by means of a continuous wire array.

In this paper, the design of the unit cell based on dipoles (or short wires) and continuous wires is presented. Each element of the cell, i.e., one dipole, two parallel dipoles and two dipoles and a wire, has been analysed in terms of transmission response and dispersion diagram. As it will be shown, this cell presents pass bands and stop bands properties at which the power will be transmitted or reflected respectively. This property has been use to create a superstrate or meta-surface configuration with a dipole tuned to its pass band, what enhances the overall radiation properties. Designing a substrate with the stop band tuned to the pass band of the superstrate, the radiation properties will be even improved; especially an important reduction of the back radiation will be achieved.

2. DESIGN OF THE UNIT CELL

As it has been commented, the design of the unit cell has been done step by step. First of all, a unit cell formed by one dipole will be analysed. Then, the properties of a unit cell formed by two dipoles and finally, a unit cell formed by two parallel dipoles and a continuous wire, will be calculated.

2.1. One Dipole Unit Cell

As it is known, a layer of dipoles excited by an incident plane wave with the E field parallel to the dipoles presents a stop band around the resonant frequency, being transparent out of this frequency. This behaviour has been analysed in terms of the transmission response and the dispersion diagram by using the software Ansoft-HFSS.

The geometry of the unit cell is shown in inset Fig. 1. The length of the dipoles is L=10.11mm, the width d=1mm and the lattice constants D_x and D_y 12.11 and 4.8mm respectively. Periodic Boundary Conditions (PBC) have been applied in order to simulate an infinite slab with an incident plane wave polarized in the E_x and H_y directions.

Plotting the S parameters of this unit cell (see Fig. 1), a resonant frequency at 18 GHz which corresponds to the dipole first resonance is observed. A second resonance can be observed at 25.5 GHz which corresponds with the grating lobe that appears at f=c/D_x.

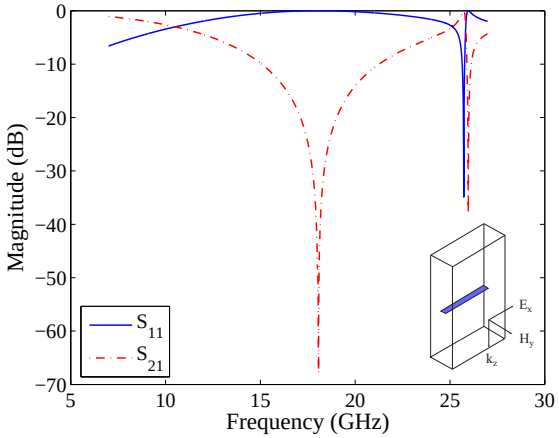

Figure 1. One-dipole unit cell. Incident plane wave analysis.

The dispersion diagram of the cell has been computed and it is depicted in Fig. 2 with the resultant irreducible Brillouin zone. Only the modes correctly polarized are shown. The periodicity in the z direction was large enough to isolate the elements, avoiding coupling effects between them. The KX section corresponds with the incident plane wave in the z direction analysed previously with the transmission response method. Similar behaviour can be observed in the dispersion diagram, where a full gap appears around the resonant frequency, from 12.76 to 24.49 GHz.

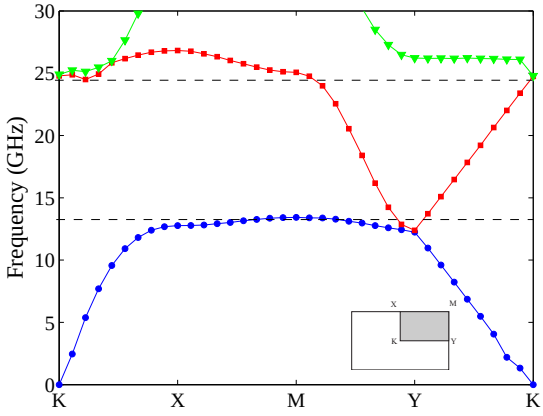

Figure 2. One-dipole unit cell. Dispersion diagram over the irreducible Brillouin zone.

2.2. Two Parallel Dipoles Unit Cell

The next step in the design of the unit cell was the analysis of a unit cell formed by two parallel dipoles (see inset Fig. 3). As in the previous case, PBC have been applied in order to simulate an infinite layer and provide the correct polarization. The dimensions of the dipoles and the lattice constants are the same than in the previous case, being the separation between dipoles h=2 mm.

For a normal incident plane wave with the electric field parallel to the dipoles and the magnetic field perpendicular to the plane which contains the pair, the electric and magnetic responses both are resonant at the same time producing a resonant behaviour of the refractive index, which can become negative above the resonance. This resonance can be understood as a resonance of a LC circuit, with the metal dipoles providing the inductance L and the dielectric gaps between the dipoles acting as capacitive elements C. Furthermore, this pair of dipoles is similar to a rectangular-double-cut split ring resonator (SRR) which arms have been stretched. So, the known equivalent LC circuit can be applied.

As in the previous case of the one dipole unit cell, the transmission response and dispersion diagram have been analysed. Computing the S parameters for the unit cell (see Fig. 3), a pass band appears at 11.87 GHz, below the stop band, due to the resonance of the structure. Analyzing the dispersion diagram (see Fig. 4), this pass band is reflected in a new mode with negative slope that appears in the KX section around the resonant frequency, which confirm the negative behaviour of the unit cell. The full gap still remains up to 25 GHz where the grating lobe appears.

Plotting the currents in the dipoles at the pass band frequency of the cell, it is observed that they are flowing in the opposite direction in both dipoles (see Fig. 5).

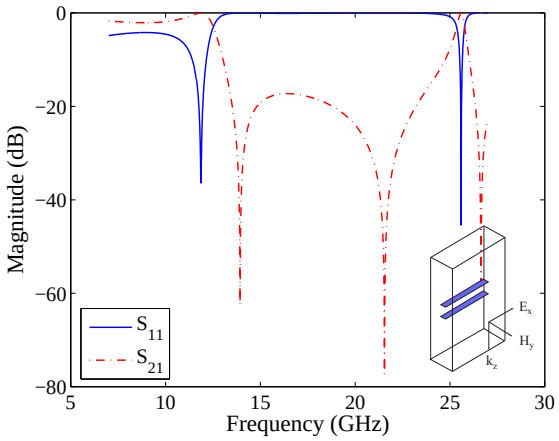

Figure 3. Two-dipoles unit cell. Incident plane wave analysis.

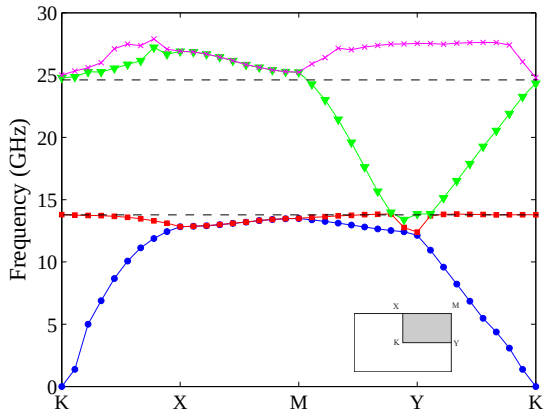

Figure 4. Two-dipoles unit cell. Dispersion diagram over the irreducible Brillouin zone.

The same result is obtained for the currents of the second mode, which confirm the correspondence between the pass band and the second mode. As in the case of the SRR, due to the small gap between dipoles, these currents are closed forming a circular path through the dipoles which leads to a magnetic field opposing the external magnetic field. As a result, the electric and magnetic resonances are obtained simultaneously and therefore the left-handed behaviour.

2.3. Two Parallel Dipoles and Wire Unit Cell

Finally, the whole unit cell formed by the two parallel dipoles and a wire has been analysed. A detail of the geometry is shown in Fig. 6. As it has been explained, the

Figure 5. Currents at the resonant frequency of the cell.

pair of dipoles is similar to a SRR. So, with the addition of the wire, this unit cell is similar to the classical SRR, shown in Fig. 6 (e).

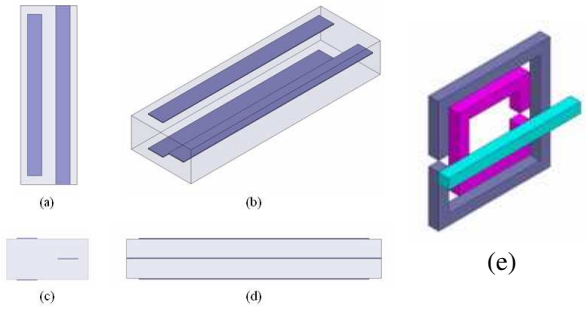

Figure 6. Two dipoles and wire unit cell. (a) E-H plane. (b) Perspective. (c) k-H plane. (d) k-E plane. (e) Classical LH unit cell.

Applying the same process than in the previous cases, the transmission response and the dispersion diagram have been calculated. Due to the presence of the wire, a new resonant frequency appears at 10.23 GHz (see Fig. 7), but the second resonance and the stop band remain unaffected. Both resonant frequencies depend on the parameters of the cell (with and lattice constants) and can be adjusted to be in close proximity in order to increase the transmission bandwidth.

This behaviour is also reflected in the dispersion diagram (see Fig. 8). In this case, two modes are present in the KX section (normal incident plane wave regime) which correspond with the two resonant frequencies, and a gap from 13.78 to 24.76 GHz.

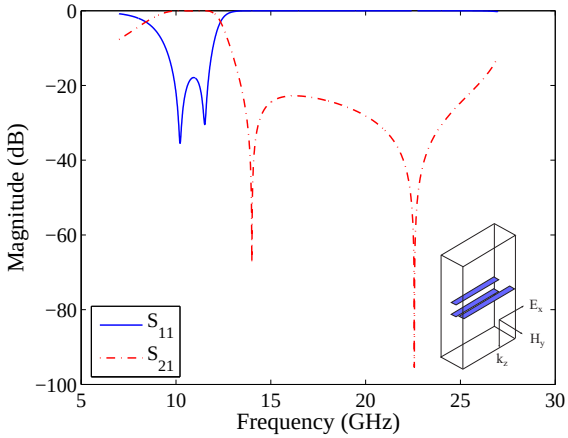

Figure 7. Two-dipoles and wire unit cell. Incident plane wave analysis.

Fig. 9 shows the currents in the dipoles and wire at both resonant frequencies. The first resonance is due to the presence of the wire. So, although both dipoles have the

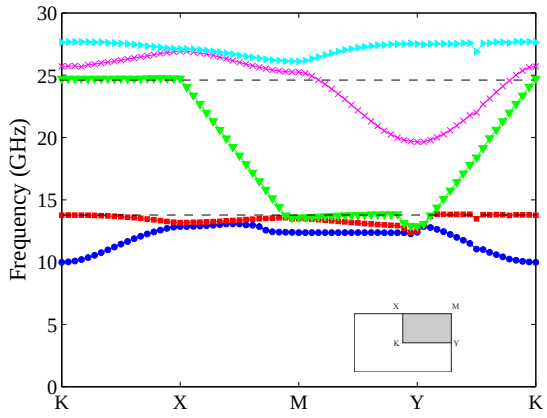

Figure 8. Dispersion diagram and the irreducible Brillouin zone.

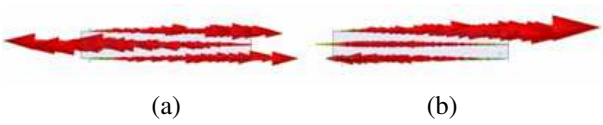

(a) (b)

Figure 9. Currents at the resonant frequency of the cell. (a) f_1 = 10.23 GHz. (b) f_2 = 11.52 GHz.

currents flowing in the same direction, the current of the wire flows in the opposite one providing the resonance of the whole structure. As it has been observed for the two-dipoles unit cell case, the second resonance is due to the electrical and magnetically excitation the parallel dipoles. So, in this case, the currents are flowing in the opposite direction creating a circular path. The same result is obtained for the currents of the two first modes, which confirm the relation between the resonant frequencies and the propagating modes.

3. SUPERSTRATE CONFIGURATION

The superstrate configuration is based on the final version of the unit cell, i.e., two parallel dipoles and a continuous wire. As it has been shown, this unit cell has a pass band and a stop band frequency. Tuning a dipole to the pass band frequency of the superstrate, the directivity and efficiency of the whole system will be enhanced.

The geometry of the structure is shown in Fig. 10. The length of the dipoles is L=9.17 mm, the thickness of the dipoles and wires d=0.8 mm, the dielectric constant ε_r=2.2, the copper cladding t=17 m, the distance between dipoles and wires d_y=0.8 mm, the horizontal distance between dipoles d_x=1 mm, the vertical distance h=1.574 mm and distance from the dipole to the superstrate 1.016 mm. The thickness of the whole configuration is 2.625 mm, i.e., less than $\lambda_0/11$ at the resonant frequency of 10 GHz. The physical area of the meta-surface is 31.51 mm x 11.2 mm, i.e., 0.39 λ_0^2 at 10 GHz. .

The whole radiating system has been analysed in terms of

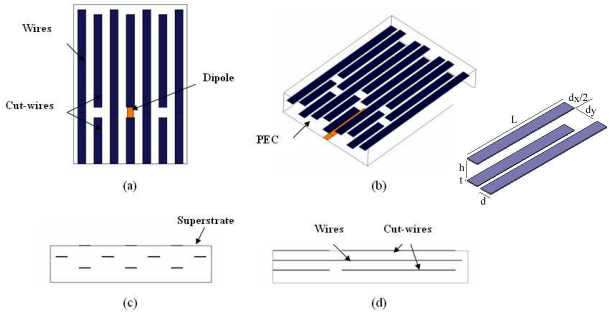

Figure 10. Superstrate configuration. (a) Top view. (b) Perspective. (c) H plane view. (d) E Plane view.

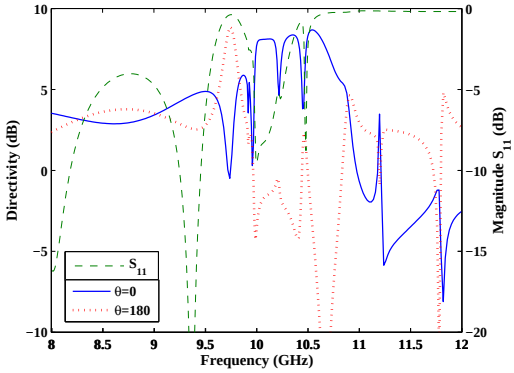

Figure 11. Directivity at θ=0-180 and S_{11} parameter.

return losses, boresight radiation and back radiation (see Fig. 11). The dashed line represents the S_{11} parameter. A resonant frequency has been obtained at 10 GHz with an impedance matching of -10 dB. Around this resonant frequency, the directivity at boresight increases (continuous line) and the back radiation decreases (dotted line).

Plotting the radiation pattern at the resonant frequency (see Fig. 12), more directive radiation patterns compared with a single dipole are obtained with a directivity at boresight of 8 dBi and a back radiation of -3.7 dBi.

Looking at the S_{11} parameter, two resonances with high directivity are observed, the main one at 10 GHz and a

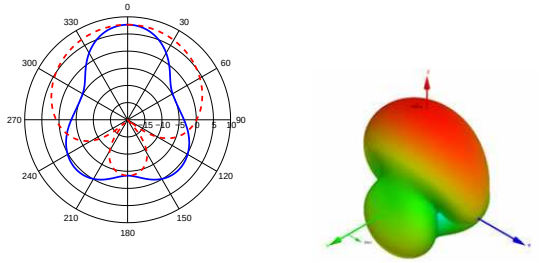

Figure 12. H-plane (continuous line) and E-plane (dashed line) and 3D radiation patterns at f_r=10 GHz.

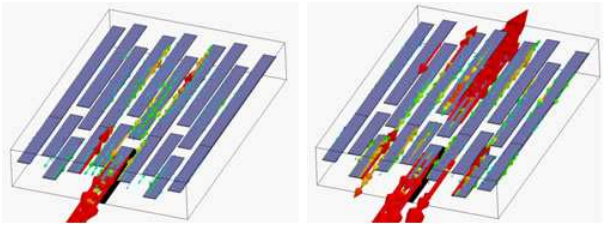

(a) (b)

Figure 13. Surface currents (a) f = 10 GHz. (b) f = 10.48 GHz.

second one at 10.48 GHz. Plotting the surface currents at these frequencies (Fig. 13 (a) and (b) respectively) it can be observed that they correspond with the two resonances obtained in the analysis of the whole unit cell. The first one is associated to the presence of the wires, with the currents in the dipoles in the same direction, and the second one is due to the dipoles, with the currents flowing in the opposite direction. As it was aforementioned and it is corroborated here, the resonance produced by the dipoles is very week, being necessary the presence of the wires.

Taking into account the physical area of the meta-surface A_{phy}, the wavelength λ_0 and the directivity D, the aperture efficiency η_{ap} can be calculated by applying (1).

$$D = \frac{4\pi}{\lambda_0^2}\eta_{ap}A_{phy} \qquad (1)$$

The directivity achieved at the first resonance of 10 GHz was 8 dBi, which means an aperture efficiency η_{ap} = 1.28. The maximum directivity was obtained around the second resonance, 8.684 dB at 10.54 GHz, i.e., η_{ap} = 1.35. These values larger than one are normal in small antennas and are included to show the good aperture efficiency that can be obtained with the presented configurations.

4. SUBSTRATE-SUPERSTRATE CONFIGURATION

As it has been seen, the unit cell also has a stop band at which the power is reflected. Tuning the stop band of the substrate to the pass band of the superstrate, the power will not be radiated to the bottom part of the structure, enhancing the directivity and reducing the back radiation. The advantage of this configuration is that it remains thin, with higher directivity and lower back radiation and better matching.

The geometry of the substrate-superstrate configuration is shown in Fig. 14. The dimensions of the superstrate are the same than in the previous case, being the dimensions of the substrate the following: L=13.6 mm, d=0.8 mm, t=17 m, d_y=2.4 mm, d_x=1.36 mm, h=1.016 mm and distance from the dipole to the substrate 0.787 mm. The thickness of the whole configuration (substrate plus superstrate) is 4.428 mm, i.e., λ_0/7 approximately at the

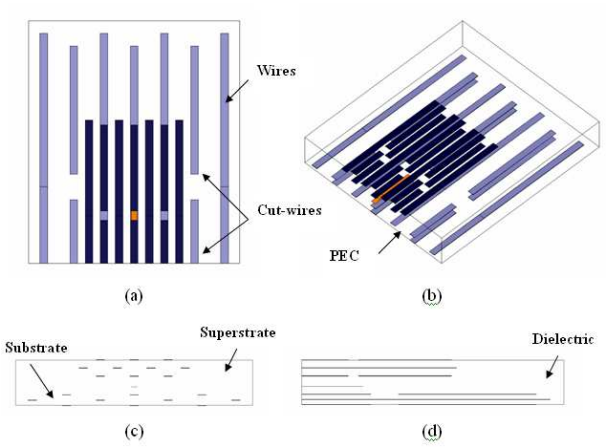

Figure 14. Substrate-superstrate configuration. (a) Top view. (b) Perspective. (c) H plane view. (d) E Plane view.

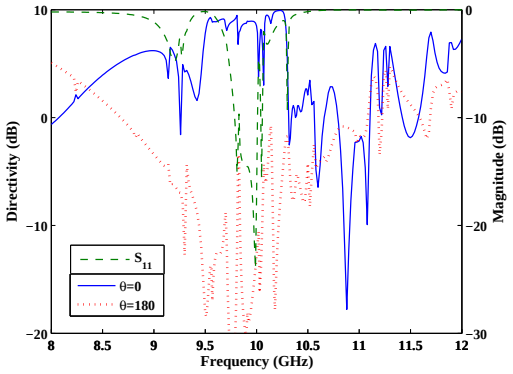

Figure 15. Directivity at θ=0-180 and S_{11} parameter.

resonant frequency of 9.99 GHz. The area of the radiating surface, the superstrate, is the same than in the previous case, 0.39 λ_0^2, but the area of the whole system (substrate and superstrate) is 1.088 λ_0^2.

As in the case of the superstrate, the S_{11} parameter, the directivity and the back radiation have been analysed (see Fig. 15). Due to the presence of the substrate, the impedance matching has improved significantly, obtaining a S_{11} value of -24 dB at the resonant frequency of 9.99 GHz. Moreover, the boresight radiation and back radiation are also enhanced in a wider band, with directivity and back radiation values of 9 and -20 dBi respectively around the resonant frequency. The H and E plane radiation patterns and the 3D one at 9.9 GHz are shown in Fig. 16.

As the case of the superstrate structure, two resonant frequencies are observed at 9.9 and 10.3 GHz. Plotting the surface currents at these frequencies (see Fig. 17 (a) and (b)), both resonances can be linked to the ones observed in the analysis of the whole unit cell.

In order to calculate the aperture efficiency around these resonant frequencies, the physical area of the whole sys-

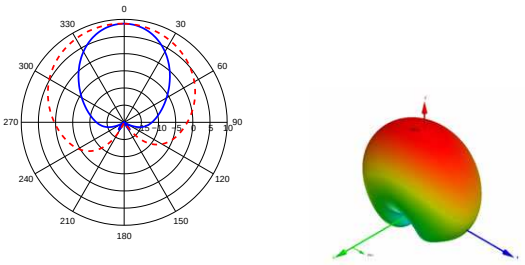

Figure 16. H-plane (continuous line) and E-plane (dashed line) and 3D radiation patterns at f=10 GHz.

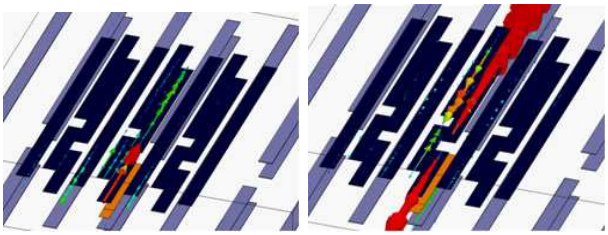

(a) (b)

Figure 17. Surface currents (a) f = 9.9 GHz. (b) f = 10.3 GHz.

tem (substrate plus superstrate) has been taken into account. However, only the superstrate is radiating, so, the aperture efficiency obtained is smaller than in the previous case. The maximum directivity obtained around the resonant frequencies was 9 dBi at 9.9 GHz and 9.934 dBi at 10.23 GHz (see Fig. 16 (a)) which means an aperture efficiency of 0.58 and 0.69 respectively.

5. CONCLUSIONS

In this paper, the design of a planar unit cell based on dipoles and continuous wires is presented. The unit cell has been analysed step by step, one dipole, two dipoles and two dipoles plus wire by means of transmission response and the dispersion diagrams. Pass band and stop bands have been observed which have been used in order to create a meta-surface for a dipole antenna. Two configurations have been analysed, obtaining an enhancement of the directivity and a reduction of the back radiation. In the case of the superstrate, the maximum directivity achieved was 8.68 dBi, which means an aperture efficiency of 1.35. By adding a substrate with the stop band tuned to the pass band of the superstrate, the directivity increased up to 9.93 dBi and the back radiation is reduced to -24 dBi.

One of the main advantages of this configuration compared with the ones formed by SRRs, is that is based on planar technology, what simplifies the manufacturing and measuring processes, and the thinner resulted configurations.

ACKNOWLEDGMENTS

The research presented in this paper has been financially supported by METAMORPHOSE NoE funded by E. C. under contract NMP3-CT-2004-50252 and the Spanish Ministry of Science and Technology under contract TIC2003-09317-c03-01.

REFERENCES

[1] Veselago V. G. *Sov. Phys. Uspekhi*, 10:509–514, 1968.

[2] Smith D. R., Padilla W. J., Vier D. C., Nemat-Nasser S. C., and Schultz S. *Phys. Rev. Lett.*, 84:4184–4187, 2000.

[3] J. B. Pendry. Negative refraction makes a perfect lens. *Phys. Rev Lett.*, 85:3966–3969, Oct. 2000.

[4] Shalaev V. M., Cai W., Chettiar U. K., Yuan H., Sarychev A. K., Drachev V. P., and Kildishev A. V. *Optics Letters*, 30:3356–3358, 2005.

[5] Zhou J., Zhang L., Tuttle G., Koschny T., and Soukoulis C. M. *Physical Review B*, 73:041101 1–4, 2006.